Journal of the Korean Physical Society, Vol. 67, No. 7, October 2015, pp. 1150∼1157

Multiplicity and Entropy Scaling of Medium-energy Protons Emitted in Relativistic Heavy-ion Collisions

A. Abdelsalam
Physics Department, Faculty of Science, Cairo University, Cairo, Egypt

S. Kamel* and M. E. Hafiz
Physics Department, Faculty of Education, Ain Shams University, Cairo, Egypt

(Received 5 June 2015, in final form 17 August 2015)

The behavior and the properties of medium-energy protons with kinetic energies in the range 26 − 400 MeV is derived from measurements of the particle yields and spectra in the final state of relativistic heavy-ion collisions (^{16}O-AgBr interactions at 60 A and 200 A GeV and ^{32}S-AgBr interactions at 3.7 A and 200 A GeV) and their interpretation in terms of the higher order moments. The multiplicity distributions have been fitted well with the Gaussian distribution function. The data are also compared with the predictions of the modified FRITIOF model, showing that the FRITIOF model does not reproduce the trend and the magnitude of the data. Measurements of the ratio of the variance to the mean show that the production of target fragments at high energies cannot be considered as a statistically independent process. However, the deviation of each multiplicity distribution from a Poisson law provides evidence for correlations. The KNO scaling behavior of two types of scaling (Koba−Nielsen−Olesen (KNO) scaling and Hegyi scaling) functions in terms of the multiplicity distribution is investigated. A simplified universal function has been used in each scaling to display the experimental data. An examination of the relationship between the entropy, the average multiplicity, and the KNO function is performed. Entropy production and subsequent scaling in nucleus-nucleus collisions are carried out by analyzing the experimental data over a wide energy range (Dubna and SPS). Interestingly, the data points corresponding to various energies overlap and fall on a single curve, indicating the presence of a kind of entropy scaling.

PACS numbers: 25.75.-q, 25.75.Gz, 25.70.Mn, 25.70.Pq, 29.40.Rg
Keywords: Nucleus-nucleus collisions, Target fragments, Multiplicity moments, Multiplicity distributions, KNO-scaling
DOI: 10.3938/jkps.67.1150

I. INTRODUCTION

Multiparticle production (MP) is an important experimental phenomenon in high-energy nucleus-nucleus (AA) collisions [1, 2]. The history MP investigation is very interesting. It is connected on the one hand with the developing theory and on the other hand with the increasing energy of accelerators. In this regard, most features of MP, such as the average charged particle multiplicity and the particle densities, are of fundamental interest as their variations with the collision energy, impact parameter and the collision geometry are very sensitive to the underlying mechanism involved in the nuclear collisions. The energy-independent KNO (Koba-Nielsen-Olesen) scaling function [3] is a good measure for the study of the MP mechanism. In the recent past, the hypothesis of KNO scaling became the dominant framework for studying experimentally [4] and theoretically [5] the behavior of the multiplicity distribution of secondary hadrons produced in hadron-hadron and hadron-nucleus collisions at high energy.

The scaling represents independence of a scaling function from the collision energy, the types of the inclusive hadrons, and their production angles and includes spectra for various selection criteria with different charged multiplicities [6]. The general principles can be applied to the AA interactions as well. Various analyses have been carried out on the produced pions. Although very little work has been done with fast target recoil protons, which are also supposed to carry information about the interaction dynamics because the time scale of emission of these particles is the same ($\approx 10^{-22}$ s) as that of the produced particles. These target fragments, which are known as grey-track particles in nuclear emulsion, are the low-energy part of the intranuclear cascade formed in high-energy interactions.

The main goal of the present investigation is to study

*E-mail: sayedks@windowslive.com

the distributions of medium-energy protons emitted in the interactions of ^{16}O-AgBr at 60 A and 200 A GeV and ^{32}S-AgBr at 3.7 A and 200 A GeV. We have compared our experimental results with the results obtained from the analysis of the data generated by using the modified FRITIOF model [7]. The validity of two types of scaling laws (KNO scaling [3] and Hegyi scaling [8]) for the experimental data is examined as well. In our earlier publication [9], we also performed similar investigations in the case of black multiplicity for these interactions. Finally, we study of the entropy production and the subsequent scaling in AA collisions by analyzing the experimental data over a wide range of incident energies.

II. KNO-SCALING FORMULAE

In 1969, Feynman [10] concluded that the mean total number of particles increases logarithmically with increasing the collision energy $\sqrt{s}$. He argued that the probability of finding a particle of type i, mass m, transverse momentum p_t, and longitudinal momentum p_z had the form

$$P_i(p_T, p_z, m) = f_i(p_T, p_z/W)\frac{dP_z d^2p_T}{E}, \quad (1)$$

where the energy of the particle E and the parameter W is given by

$$E = \sqrt{m^2 + p_T^2 + p_z^2} = \sqrt{m_T^2 + p_z^2} \text{ and } W = \frac{\sqrt{s}}{2}. \quad (2)$$

The function $f_i(p_T, p_z/W)$ is a structure function and is known as the Feynman function. Feynman's assumption was that f_i was independent of W, which is called Feynman scaling.

If the invariant cross section, σ, is used, the integration of Eq. (1) under the assumption Feynman made (W is large) can give the mean multiplicity in the form

$$< n > \ \propto \ \ln(W) \ \propto \ \ln\sqrt{s}. \quad (3)$$

The concept of Feynman scaling was the main assumption when Koba, Nielsen, and Olesen suggested a similar scaling in 1972 [3]. This scaling is now called KNO scaling.

One of the most influential contributions to the analysis of multiplicity distributions was made by KNO. They put forward the hypothesis that at very high energies, the probability distributions $P(n)$ for detecting n final state particles exhibit a scaling law of the form

$$P(n) = \frac{1}{< n >}\psi(z) = \frac{\sigma_n}{\sigma_{inel}}. \quad (4)$$

The variable $z = n/ < n >$ stands the for normalized multiplicity, $< n >$ represents the average number of charged secondary particles, σ_n is a partial cross-section for producing n charged particles and σ_{inel} is the total inelastic cross-section. That is to say, the $< n > P(n)$ measured at different energies (*i.e.*, $< n >$ scales to the universal curve ψ when plotted against the multiplicity n rescaled by the average multiplicity $< n >$. The scaling function $\psi(z)$ must satisfy the normalization conditions

$$\int_0^\infty \psi(z)dz = \int_0^\infty z\psi(z)dz = 1, \ \ (i.e., < z >= 1). \quad (5)$$

As the multiplicity increases, the fluctuations increase accordingly. To normalize the fluctuations from naively increasing in multiplicity, we define the normalized standard moments M_q as

$$M_q = \frac{< n^q >}{< n >^q}, \quad (6)$$

where $q = 2, 3, 4 \cdots$. Obviously, the standard moments M_q of $\psi(z)$ are independent of the collision energy if Eq. (4) is satisfied.

Besides $\psi(z)$, a second properly-normalized scaling function is obeyed by $P(n)$. Hegyi [8] demonstrated that in addition to $< n > P(n)$, the more simple combination $nP(n)$ also scaled to a universal curve in the variable $n/ < n >$ if KNO scaling is valid. This yields the scaling law for the multiplicity distributions (MDs) in the form

$$\varphi(z) = nP(n). \quad (7)$$

The obvious advantages of this new scaling are as follows: (i) $nP(n)$ is not influenced by statistical and systematic uncertainties in $< n >$; hence, $\varphi(z)$ provides more selective power than the original KNO-scaling function $\psi(z)$. (ii) The new scaling function generates a scale parameter $\sigma = 1$ because it depends only on the combination of z and the scale parameter of $\psi(z)$.

III. EXPERIMENTAL DETAILS

Two stacks of nuclear emulsions were horizontally exposed to ^{32}S beams at two widely differing energies. The first stack of Br-2 emulsion pellicles was irradiated at 3.7 A GeV at the Dubna Synchrophasatron, and the second one of FUJI films was exposed to 200 A GeV at the CERN-SPS (Exp. no. EMU03). Additionally, two stacks of nuclear emulsions were horizontally exposed to ^{16}O ion beams at the CERN SPS. The first stack of the FUJI films was irradiated at 60 A GeV and the second one of the ILFORD−G5 was exposed to 200 A GeV. The chemical compositions of the used emulsion types are shown in Table 1.

The pellicles were scanned under 100× magnifications with an "along-the-track" scanning technique. Each beam track was carefully followed up to a distance of 5 cm or until it interacted with an emulsion nucleus. Other details of the irradiations and the scanning are given in

Table 1. Chemical composition of the used emulsion types (atoms/cm^3 $\times$ 10^{22}).

Element	^{1}H	^{12}C	^{14}N	^{16}O	^{32}S	^{80}Br	^{108}Ag	^{133}I
NIKFI-BR2	3.1500	1.4100	0.3950	0.9560	-	1.0280	1.0280	-
FUJI	3.2093	1.3799	0.3154	0.9462	0.0134	1.0034	1.0093	0.0055
ILFORD-G5	3.1900	1.3900	0.3200	0.9400	0.0140	1.0100	1.0200	0.0060

earlier publications [9, 11–13]. At all energies, all samples with inelastic interactions with emulsion nuclei were analyzed by studying the tracks emitted from each interaction detected. Depending on the commonly-accepted emulsion experiment terminology [14], we classified the tracks of secondary charged particles generated in each interaction according to their ionization, range and velocity as follows:

(a) Black (b) particles are those having a range of $L <$ 3 mm, corresponding to protons with kinetic energies $\leq$ 26 MeV. They are mainly due to evaporated target fragments. Their multiplicity is denoted as n_b.

(b) Gray (g) particles have a range $L \geq 3$ mm in the emulsion. These tracks are mostly due to protons with kinetic energies in the range $26 - 400$ MeV. Their multiplicity is denoted as n_g. In each event, the black and the gray tracks together are called heavily-ionizing tracks. Their multiplicity is denoted as $n_h = n_g + n_b$.

(c) Shower (s) particles are singly-charged relativistic particles that mainly consist of pions. Their multiplicity is denoted as n_s.

An event-by-event analysis demands the separation of events into ensembles of collisions of different projectiles with hydrogen (H), light nuclei (CNO) and heavy nuclei (AgBr). Usually events with $n_h \leq 1$ are classified as collision with hydrogen. Events yielding two to seven heavy tracks are classified as CNO events. Events with $n_h \geq 8$ arise from collisions with heavy nuclei. In this method the separation of events for an AgBr target is quite accurate in samples with $n_h \geq 8$, but in samples with $2 \leq n_h \leq 7$, there is an admixture of CNO events and peripheral collisions with the AgBr target. In this work, only events with a number of heavy tracks $n_h \geq 8$ were selected so as to exclude CNO interactions and peripheral collisions with the AgBr target [15].

IV. EXPERIMENTAL RESULTS

In this work, the modified FRITIOF code (MFC) used is based on the earliest version of the FRITIOF code (version 1.6) [16]. The modification was carried out by Shmakov and Uzhinskii [7]. Running the encoded simulation for different emulsion types (see Table 1), we simulated the probabilities of collisions with different components of the nuclear emulsion according to Glauber's approach [7]. Then, the FRITIOF simulations were run.

1. Higher-order Multiplicity Moments of Grey Particles

The usual method of investigating the charged-particle multiplicity distribution and its shape is to calculate its higher moments. Higher moments, which have become very popular nowadays, are much more sensitive not only to physics effects but also to statistical fluctuations. Recently, the beam-energy and the system-size dependences for higher moments of net-charge and net-proton MDs in AA interactions at different beam energies have been studied in Refs. [17] and [18]. In statistics, probability distribution functions can be characterized by using moments of various orders [19], such as the mean, $M = < n >$, the variance, $\sigma^2 = < (\Delta n)^2 >$, the skewness $Skew = < (\Delta n)^3 > /\sigma^3$, and the Kurtosis $K = < (\Delta n)^4 > /\sigma^4 - 3$, where $\Delta n = n - < n >$. Collectively, all moments contain information on the full distribution, but in practice, only the first few moments can be calculated with reasonable uncertainties due to limited statistics.

Skewness and kurtosis are widely used to characterize the properties of probability distributions. Skewness which is used to describe the asymmetry property of distributions can come in the form of "negative skewness" or "positive skewness", depending on whether data points are skewed to the left (negative skew) or to the right (positive skew) of the data average. On the other hand, in statistics, kurtosis is the degree of flatness or 'peakedness' in the region of the mode of a frequency curve. That is, kurtosis quantifies whether the shape of the data distribution matches the Gaussian distribution. It is measured relative to the 'peakedness' of the normal (Gaussian) curve and tells us the extent to which a distribution is more peaked or flat-toped than the normal curve. If the curve is more peaked than a normal curve, it is called Leptokurtic (more than 3). In this case, items are more clustered about the mode. If the curve is more flat-topped than the normal curve, it is Platykurtic (less than 3). The normal curve itself is known as Mesokurtic

Table 2. Experimental mean values as well as the variance, skewness, kurtosis and the scaled variance (ratio of variance to mean), for the g-particles and the corresponding values calculated by using the MFC.

Interaction	Energy (A GeV)	$< n_g >$	$< n_g >_{MFC}$	Variance (σ^2)	Skewness ($Skew$)	Kurtosis (K)	$\sigma^2/ < n_g > (\omega)$
^{32}S-AgBr	3.7	7.15 ± 0.41	11.04	18.53 ± 1.72	0.89 ± 0.54	3.62 ± 1.07	2.59 ± 0.80
^{32}S-AgBr	200	4.75 ± 0.23	9.87	9.04 ± 1.63	0.96 ± 0.63	3.55 ± 1.27	1.90 ± 0.36
^{16}O-AgBr	60	5.56 ± 0.29	8.17	13.53 ± 1.11	0.98 ± 0.55	3.52 ± 1.10	2.13 ± 0.21
^{16}O-AgBr	200	5.01 ± 0.30	8.25	9.61 ± 1.29	0.95 ± 0.63	3.58 ± 1.27	1.92 ± 0.28

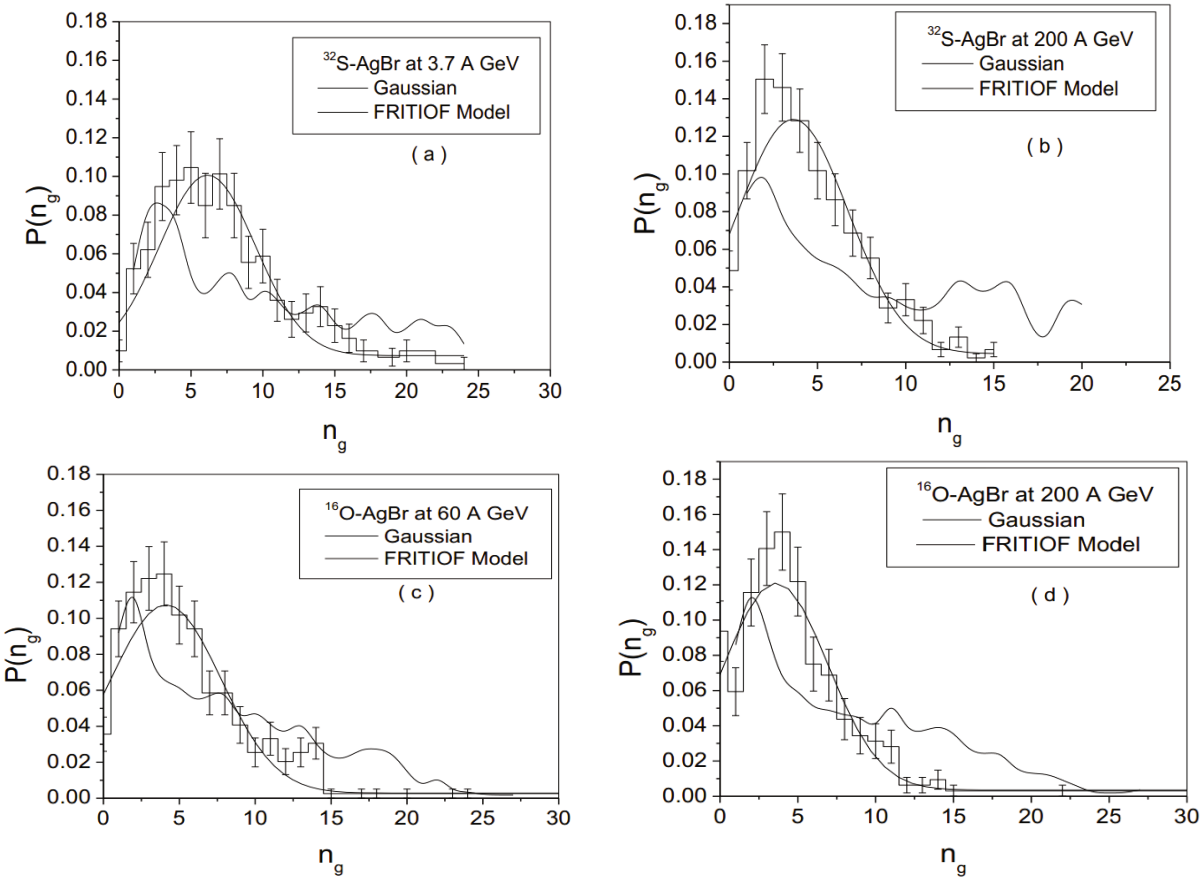

Fig. 1. MDs of g-particles fitted with a Guassian distribution and the predictions of the MFC in the collisions of ^{32}S-AgBr at (a) 3.7 A and (b) 200 A GeV, as well as in the collisions of ^{16}O-AgBr at (c) 60 A and (d) 200 A GeV.

(equal to 3). The measure of kurtosis is very helpful in the selection of an appropriate average [20]. For example, for a normal distribution, the mean is most appropriate, for a leptokurtic distribution, the median is most appropriate, and for a platykurtic distribution, the quartile range is most appropriate.

For Gaussian distributions, the skewness and excess kurtosis (= kurtosis − 3) are equal to zero. Thus, they are an ideal probe to demonstrate the non-Gaussian fluctuation feature. Recently, the results obtained in Ref. [21] made possible a rather simple way to perform mathematical and computer simulations of non-Gaussian distributions with zero skewness and kurtosis in solving the problems of measurements, detection, and classification.

In Table 2, we display the general characteristics of the g-particle multiplicity distribution emitted in the ^{32}S-AgBr interactions at 3.7 A and 200 A GeV and in the ^{16}O-AgBr interactions at 60 A and 200 A GeV by using the higher-order moments [19], such as the mean $< n_g >$, the variance σ^2 which estimates the dispersion of the data about the mean, the skewness $Skew$ which measures how symmetric the distribution is, and the kurtosis K which measures how sharply peaked the distribution is. The results in Table 2 show that the distributions are positively and moderately skewed, meaning that the

Table 3. Parameters and χ^2/DoF of the Gaussian fits to the MDs for g-particles.

Interaction	Energy (A GeV)	Width	Peak	Central value	χ^2/DoF
^{32}S-AgBr	3.7	6.68 ± 0.52	0.10	6.15 ± 0.26	0.08
	200	6.25 ± 0.46	0.13	3.62 ± 0.22	0.11
^{16}O-AgBr	60	7.27 ± 0.55	0.11	4.13 ± 0.28	0.09
	200	6.66 ± 0.59	0.12	3.60 ± 0.31	0.07

right tail of each distribution is longer than the left tail. Also, the slightly positive values of the kurtosis indicate the possibility of a slightly leptokurtic distribution.

An event-by-event measurement of the anisotropy in heavy-ion collisions is expected to yield fluctuations from different sources [22]. As a measure of multiplicity fluctuations among the emitted fragments, we use here, as in the study described in Ref. 9, the scaled variance ω $(= \sigma^2/ < n_g >)$ of the multiplicity distribution of g-particles. The measured values of ω in Table 2 show that the MDs in the present work are not Poissonian ($\omega > 1$).

2. Multiplicity Distributions

In Fig. 1, the normalized MD of g-particles is fitted with a Gaussian distribution in the ^{32}S-AgBr interactions at (a) 3.7 A and (b) 200 A GeV as well as in the 16O-AgBr interactions at (c) 60 A and (d) 200 A GeV. A comparison with the predictions from the modified FRITIOF model is performed as well in Fig. 1. For the former case, the parameter values for each Gaussian fit and the corresponding χ^2/Degree of Freedom (DoF) are calculated, as demonstrated in Table 3. The MDs of g-particles for all interactions are seen to have been fitted well with the Gaussian distribution function. For the latter case, however, noticeable from Table 2 is the fact that the mean multiplicity for all interactions calculated by using the FRITIOF model was larger than it was in experimental distribution. In addition, generally, the predictions of the MFC in the region of $n_g \leq 10$ underestimate the g-particle production and vice versa in the region of $n_g > 10$. Clearly in all interactions, the modified FRITIOF model does not describe the target fragmentation region sufficiently well. The comparison indicates a need to modify the code to give reasonably accurate rescattering.

3. Scaling and Entropy

In Fig. 2(a), the KNO scaling function $< n > P(n) = \psi(z)$ for g-particle multiplicity data at different energies

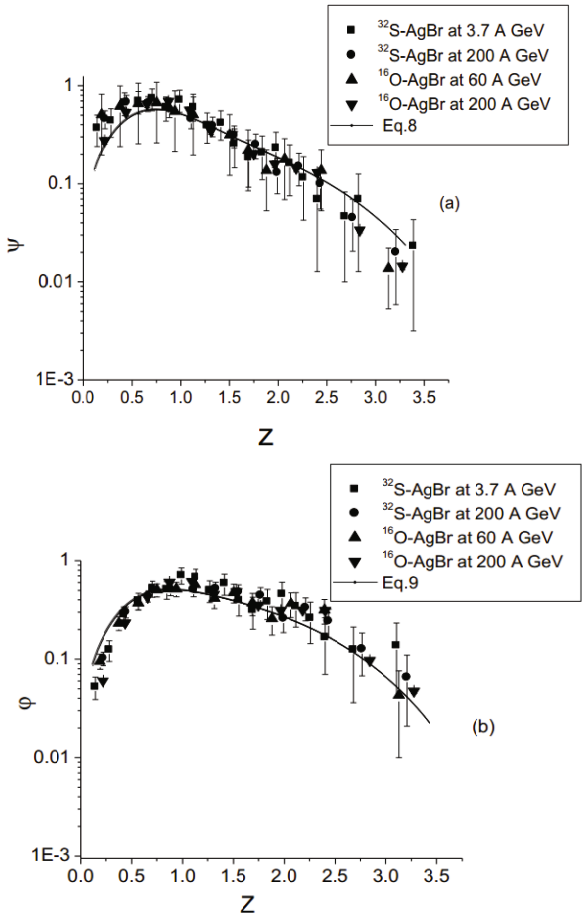

Fig. 2. (a) KNO scaling function $< n > P(n) = \psi(z)$ and (b) KNO scaling function $nP(n) = \varphi(z)$ for g-particle multiplicity data at different energies fitted with Eqs. (8) and (9), respectively.

is fitted with the function (solid curve)

$$\psi(z) = (1.66z + 16.96z^3 - 3.96z^5 + 1.68z^7 - 0.09z^9) \times \exp(-3.44z). \quad (8)$$

The value of χ^2/DoF is 0.03. Thus, we can see that our experimental data are consistent with the KNO-scaling hypothesis. In Fig. 2(b), the KNO scaling function $nP(n) = \varphi(z)$ for g-particle multiplicity data at dif-

ferent energies is fitted with the function

$$\varphi(z) = (1.01z + 13.26z^3 - 1.03z^5 + 1.57z^7 - 0.10z^9) \times \exp(-3.36z). \quad (9)$$

The scaling function $\varphi(z)$ represented by the solid curve approximately reproduces the MD of g-particles for all the interactions with a $\chi^2/\mathrm{DoF} = 0.03$. The error bars are drawn for every experimental point. The errors shown in Fig. 2 are purely statistical. Investigating $nP(n)$ instead of $< n > P(n)$ has the obvious advantage that the statistical and the systematic errors of $< n >$ do not contribute to the experimental uncertainty in the shape of the scaling function. Therefore, $\varphi(z)$ can be more selective between various theoretical predictions than $\psi(z)$ [8].

Previously [23], the analysis of the *p*-*p*, *d*-*d* and *a*-*a* data in terms of multiple nucleon-nucleon collisions was most convenient when Gamma distributions were used to represent the spectral shapes. This property is also known as KNO scaling. In this context, because the gamma distribution has a scaling property (that is, if $\psi(z) \sim$ gamma(θ, k) with a scale parameter θ and a shape parameter k, then $\varphi(z) = z\psi(z)$ also has the gamma distribution), Hegyi proposed a form for the scaling function by using a new scaling variable $\omega = z\theta$, which is given in Ref. [8] by Eq. (15):

$$\varphi(\omega) = \omega^k \exp(-\omega)/\Gamma(k). \quad (10)$$

It is tempting to check the validity of Eq. (10) against the data shown in Figs. 2(a) and (b). Accordingly, the solid curves in Figs. 3(a) and (b) represent the theoretical $\psi(z)$ and $\varphi(z)$, respectively, corresponding to Eq. (10). The results lend support for the validity of the above scaling (Eq. 10).

Obviously, the moments M_q of $\psi(z)$ are independent of the collision energy as long as the KNO form is valid. Thus, the moments of the two KNO-scaling functions are related by

$$M_q^{\varphi} = M_{q+1}^{\psi}. \quad (11)$$

The values of the moments in Table 4 satisfy the equality in Eq. (11).

In high-energy heavy-ion collisions performed at energies per nucleon considerably greater than the nucleon rest mass, the final state contains a large amount of entropy related to multiparticle production, as compared to N−N reactions, and to their spectral distributions, which are of a thermal character. An entropy measurement in AA collisions may serve as a tool to investigate correlations and event-by-event fluctuations. However, we study here the energy dependence of the multiplicity by estimating the entropy production in multiparticle systems, which is defined by Simak *et al.* [24] as

$$S = -\sum_n P(n) \ln P(n), \quad (12)$$

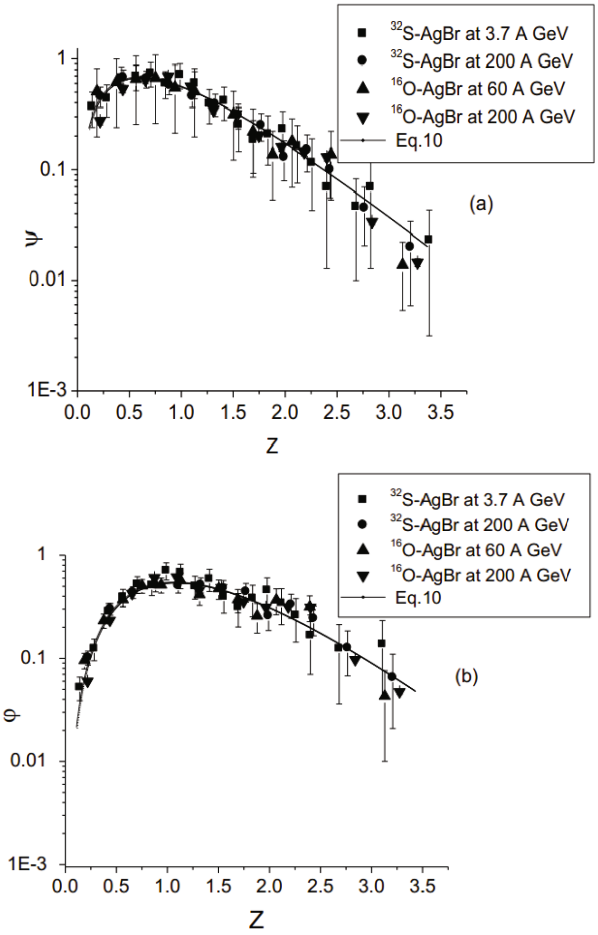

Fig. 3. (a) KNO scaling function $< n > P(n) = \psi(z)$ and (b) KNO scaling function $nP(n) = \varphi(z)$ for gray-particle multiplicity data at different energies. Both are fitted with Eq. (10).

where $\sum_n P(n) = 1$. A relationship exists between the entropy S, the average multiplicity $< n >$, and the KNO function $\psi(z)$, as long as the KNO form in Eq. (4) is valid. Therefore, for functions satisfying the normalization conditions in Eq. (5), the following inequality is valid:

$$\frac{S}{\ln < n >} \leq 1 + \frac{1}{\ln < n >}. \quad (13)$$

The present values of the mean multiplicity and the entropy of medium energy protons in Table 5 seem to be prove the inequality in Eq. (13). We notice that KNO scaling is equivalent to scaling with the ratio $S/\ln < n_g >$ in the asymptotic limit, and that the approach to this limit is very slow.

Finally, an attempt is made to examine the occurrence of entropy scaling with the present data over a wide energy range (Dubna and SPS). Figure 4 illustrates a plot of the behavior of the entropy S as a function of the number of the target protons, n_g, emitted in all interactions. Interestingly the data points corresponding to

Table 4. Moments of the two KNO scaling functions.

Interaction	Energy (A GeV)	M_q^{φ}				M_q^{ψ}				
		M_2	M_3	M_4	M_5	M_2	M_3	M_4	M_5	M_6
^{32}S-AgBr	3.7	2.33	4.60	9.97	23.70	1.39	2.35	4.62	10.07	23.93
	200	2.70	5.74	13.53	34.32	1.55	2.84	6.03	14.22	36.07
^{16}O-AgBr	60	2.72	5.74	13.21	32.32	1.54	2.83	5.95	13.70	33.53
	200	2.63	5.46	12.57	31.10	1.60	2.87	5.97	13.73	33.95

Table 5. Values of the mean (see Table 2) and the entropy for g-particles prove the inequality of Eq. (13).

Interaction	Energy (A GeV)	S	$S/\ln < n_g >$	$1 + 1/\ln < n_g >$
^{32}S-AgBr	3.7	2.74 ± 0.16	1.39 ± 0.08	1.51 ± 0.09
	200	2.35 ± 0.11	1.51 ± 0.07	1.64 ± 0.08
^{16}O-AgBr	60	2.57 ± 0.13	1.46 ± 0.08	1.57 ± 0.08
	200	2.35 ± 0.14	1.46 ± 0.09	1.62 ± 0.10

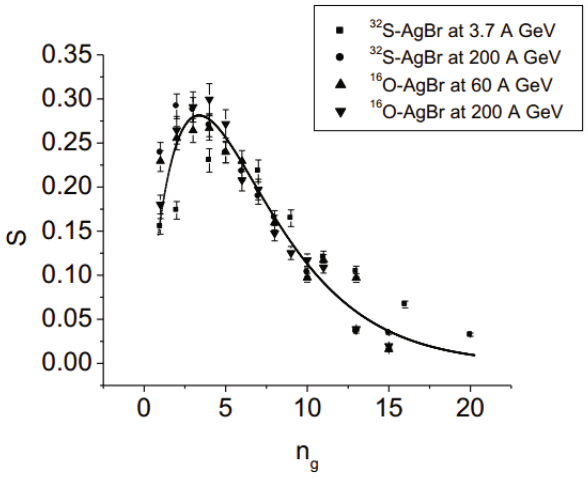

Fig. 4. Behavior of the entropy as a function of the number of target protons emitted in all interactions.

various energies overlap and fall on a single curve, indicating the presence of a kind of entropy scaling that is well fitted with the function $S = 0.232 n_g \exp(-0.303 n_g)$, with $\chi^2/\mathrm{DoF} = 0.02$.

V. CONCLUSION

Based on the findings of this study, let us summarize our main results:

1. In this work, the behavior and the properties of medium-energy protons with kinetic energies in the range 26 − 400 MeV are derived from measurements of the particle yields and spectra in the final state of relativistic heavy-ion collisions (^{16}O-AgBr interactions at 60 A and 200 A GeV and ^{32}S-AgBr interactions at 3.7 A and 200 A GeV) and their interpretations are given in terms of the higher-order moments.

2. The multiplicity distributions for all interactions are well fitted with Gaussian distribution functions. The data also are compared with the predictions of the modified FRITIOF model, showing that the predictions do not reproduce the trend and the magnitude of the data. The comparison indicates a need to modify the code to give reasonably accurate rescattering.

3. Fluctuations and correlations are second moments, so they allow for a better understanding of physical processes. The direct measure of the scaled variance ω was used as a measure of multiplicity fluctuations. The measurements ($\omega > 1$) showed that the production of target fragments at high energies could not be considered as a statistically-independent process. However, the deviation of each multiplicity distribution from a Poisson law is evidence for correlations. These correlations may be interpreted in terms of the concept of clustering [25]; that is, the particle production takes place via the formation of some intermediate states, referred to as "clusters", which finally decay isotropically in their center-of-mass (c.m.) frame to real hadrons.

4. The KNO scaling behaviors of two types of scaling (Koba−Nielsen−Olesen (KNO) scaling and Hegyi scaling) functions in terms of the multiplicity distribution were investigated. We demonstrated that besides $< n > P(n)$, the more simple combination $nP(n)$ also scaled to a universal curve in the variable $n/ < n >$ when KNO scaling was valid. A simplified universal function was used in each scaling to display the experimental data.

5. The examination of the relationship between the entropy, the average multiplicity, and the KNO function suggests that KNO scaling is equivalent to scaling of the ratio $S/\ln < n_g >$ in the asymptotic limit as long as the KNO form is valid.

6. Entropy production and subsequent scaling in AA collisions was carried out by analyzing the experimental data over a wide energy range (Dubna and SPS). Interestingly, the data points corresponding to various energies overlap and fall on a single curve, indicating the presence of a kind of entropy scaling.

Recently [9, 26, 27], the search for a scaling formula, which is universal to all types of reactions, that is, hadron−hadron, hadron−nucleus, and nucleus−nucleus interactions, has been of great importance for studying the collision dynamics involved in particle production.

ACKNOWLEDGMENTS

We owe much to the Vekseler and Baldin High Energy Laboratory, the Joint Institute for Nuclear Research (JINR), Dubna, Russia, for supplying us the photographic emulsion plates for 3.7 A GeV ^{32}S irradiated at the Synchrophasotron. We are pleased to acknowledge the kind help of the CERN authorities for providing the photographic plates for ^{16}O (60 A and 200 A GeV) and ^{32}S (200 A GeV) irradiated at the Super Proton Synchrotron (SPS).

REFERENCES

[1] J. Manjavidze and A. N. Sissakyan, Phys. Rep. **346**, 1 (2001).
[2] F. H. Liu, X. Y. Yin, J. L. Tian and N. N. A. Allah, Phys. Rev. C **69**, 034905-1(2004).
[3] Z. Koba, H. B. Nielsen and P. Olesen, Nucl. Phys. B **40**, 317 (1972).
[4] P. Slattery, Phys. Rev. Lett. **29**, 1624 (1972).
[5] W. Thane *et al.*, Nucl. Phys. B **129**, 365 (1997).
[6] M. V. Tokarev and I. Zborovsky, Phys. At. Nucl. **70**, 1294 (2007).
[7] S. Yu. Shmakov and V. V. Uzhinskii, Com. Phys. Comm. **54**, 125 (1989); Kh. El-Waged and V. V. Uzhinsky, Phys. At. Nucl. **60**, 828 (1997).
[8] S. Hegyi, Phys. Lett. B **335**, 226 (1994).
[9] A. Abdelsalam *et al.*, Int. J. Mod. Phys. E **23**, 1450040 (2014).
[10] R. P. Feynman, Phys. Rev. Lett. **23**, 1415 (1969); C. Nygaard, Niels Bohr Institute, CERN-Ph.D. thesis-2011-283.
[11] M. El-Nadi *et al.*, Int. J. Mod. Phys. E **06**, 191 (1997).
[12] A. Abdelsalam *et al.*, J. Phys. G: Nucl. Part. Phys. **28**, 1375 (2002).
[13] M. El-Nadi *et al.*, J. Phys. G: Nucl. Part. Phys. **28**, 241 (2002).
[14] C. F. Powell, P. H. Fowler and D. H. Perkins, *the Study of the Elementary Particles by the Photographic Method* (Pergamon, Oxford, 1959), p. 450 and references therein.
[15] D. Ghosh *et al.*, Int. J. Mod. Phys. E **20**, 1171 (2011).
[16] B. Nilsson-Almqvist and E. Stenlund, Computer Phys. Comm. **43**, 387 (1987).
[17] X. Wang and C. B. Yang, J. Phys. G: Nucl. Part. Phys. **40**, 075103 (2013).
[18] T. J. Tarnowsky and G. D. Westfall, arXiv:1210.8102v2 [nucl-ex] (2013).
[19] D. J. Mangeol, arXiv: 0110029 v1 [hep-ex] (2001).
[20] Lawrence T. DeCarlo, Psychol. Meth. **2**, 292 (1997).
[21] A. I. Krasil'nikov, Radioelect. Commun. Sys. **56**, 312 (2013).
[22] B. Alver *et al.*, Phys. Rev. Lett. **104**, 14 (2010).
[23] A. L. S. Angelis *et al.*, Phys. Lett. B **168**, 158 (1986).
[24] V. Simak *et al.*, Phys. Lett. B **206**, 159 (1988).
[25] A. Shakeel *et al.*, Int. J. Mod. Phys. E **8**, 121 (1999); E. L. Berger, Nucl. Phys. B **85**, 61 (1975).
[26] S. Bhattacharyya, Int. J. Mod. Phys. E **19**, 319 (2010).
[27] C. Beck, *Lecture note in physics, Clusters in nuclei V3* (Springer International, Switzerland, 2014), p. 54.